G12C: NEW CLINICAL PERSPECTIVE IN LUNG ADENOCARCINOMA

Curso: 2019/2020

Autor: Luisa Ayelen Ramos Navas
Master en Biomedicina. Universidad de La Laguna

Tutor: Eduardo Salido Ruiz
Grupo: Patología celular y Molecular

Dr Eduardo Salido componente/coordinador del Grupo de Investigación Patología celular y molecular, adscrito a la Titulación que aparece en el encabezamiento

CERTIFICO

- Que el Trabajo Fin de Máster (TFM) titulado G12 C: New clinical perspective in Lung Adenocarcinoma ha sido realizado bajo mi supervisión por Dª Luisa Ayelen Ramos Navas, matriculada en el Máster en Biomedicina, durante el curso académico 2019-2020

- Que una vez revisada la memoria final del TFM, doy mi consentimiento para ser presentado a la evaluación (lectura y defensa) por el Tribunal designado por la Comisión Académica de la Titulación.

Para que conste, firmo el presente certificado en La Laguna a 30 de junio de 2020

Dr Eduardo Salido Ruiz

ACKNOWNLEDGEMENTS

To my tutor Dr. Eduardo Salido for letting me be myself and for giving me the opportunity to carry out a project that means so much to me, to fight tirelessly against cancer, and for being a model of endeavour and sacrifice for all those who want to follow in his footsteps, but especially for teaching me to enjoy science as much as he does.

To Alba, Raquel, Agoney, Clesay, María, Neizan, Carlota, Estela and Pol for being my inspiration and the main reason for this endeavour. I just hope that one day I can give you back everything you have brought me with your smiles and desire to fight.

To the Asociación Española Contra el Cancer for allowing me to see the other side of this struggle and for the incredible work they do. Especially to my fellow volunteers for joining me in this battle and for teaching me to value the little things. And to Salka, the amazing coordinator of the hospital volunteers, for not only supporting me every step of the way but also for teaching me to look beyond research; for inspiring me to be a better person with every act, with every experiment and at every moment of the day.

And finally, to my family, for their unconditional support. For awakening in me, the little girl that I was, a passion for science and teaching me the importance of helping others. For saying the right words at the right time and for always being with me at every step.

None of this would have been possible without all of you. Thank you.

INDEX

ABSTRACT

KRAS activating mutations are among the most frequent drivers in human cancer. However, the published series addressing the prevalence of KRAS G12C in lung adenocarcinoma are few and controversial. The objective of this study is to establish the prevalence of KRAS G12C mutation in lung adenocarcinoma as well as its possible coexistence with mutations in EGFR, ALK and BRAF. Also studying a possible morphological correlation with mutations in KRAS.

Three hundred consecutive lung adenocarcinoma stage IIIb and IV cases diagnosed at the Dept. Pathology, Hospital Universitario de Canarias were included. Tumor genotyping was performed using the KRAS pyrosequencing kit (Qiagen).

KRAS was mutated in approximately 35% of cases, being KRAS G12C the most frequent mutation. Mutated adenocarcinomas of KRAS could be seen also carrying mutations in EGFR or BRAF V600E. However, none was associated with ALK translocation. Therefore, KRAS mutations do not appear to be mutually exclusive with EGFR or BRAF mutations.

No statistically significant association between histology subtypes of lung adenocarcinoma and mutations in KRAS was found, not even the mucinous phenotype, which has been suggested to harbor KRAS mutations in a higher proportion (p=0,318).

Due to the recent development of KRAS inhibitors, it seems necessary to genotype KRAS in lung adenocarcinomas using protocols that can distinguish specific alleles since the therapy currently in clinical trials is mutation-specific. Pyrosequencing is a simple, low-cost and fast genopyting method for this purpose.

Keywords: Adenocarcinoma; mutations; KRAS; G12C; EGFR; BRAF; ALK; ROS1.

ABBREVIATIONS

ADC	Adenocarcinoma
ALK	Anaplastic lymphoma receptor tyrosine kinase
DNA	Deoxyribonucleic acid
EGFR	Epidermal growth factor
GDP	Guanosine diphosphate
GTP	Guanosine triphosphate
G12A	Glycine 12 Alanine
G12C	Glycine 12 Cisteine
G12D	Glycine 12 Aspartic
G12R	Glycine 12 Arginine
G12S	Glycine 12 Serine
G12V	Glycine 12 Valine
MAPK	Mitogen activated protein kinase
MEK	Mitogen Activated Protein kinase
NGS	Next generation sequencing
RAF	Rapidly accelerated fibrosarcoma
PCR	Polymerase chain reaction
RAS	Rat sarcoma
TKI	Tirosin kinase inhibitor

1. INTRODUCTION

1.1. Lung Cancer

Lung cancer is the leading cause of death worldwide. In Spain, in 2019, 27,939 new cases of lung cancer were registered, and 22,569 patients died from this cause. The incidence of this disease is expected to increase in the future with an estimated 110,350 deaths in 2040. The lack of specific signs and symptoms, as well as the failure of screening methods result in a delayed diagnosis and a large number of advanced stages at the time of recognition (Domagala-Kulawik, 2019).

For many years, lung cancer was classified histologically as "small cell" and "non-small cell" lung cancer and this classification was the basis of treatment. With the recent development of personalized medicine and targeted therapies, this simplified stratification scheme has been revised in order to establish a more specific subtype within the group of non-small cell lung carcinoma (NSCLC) (Domagala-Kulawik, 2019).

The discovery of specific genetic alterations made necessary to review the previous approach, gradually leading to the development of a molecular genetic classification for lung tumors. Currently, NSCLC is divided into two main subtypes, squamous cell carcinoma (SQCC) and adenocarcinoma (ADC) which is the most frequent (38% of lung cancers) and the type in which this study will focus on. Although lung cancer is associated with tobacco, an increasing number of nonsmokers and never smokers are developing lung adenocarcinoma. These two types of lung cancer differ not only in their histology and molecular pattern, they are also susceptible to different therapies. (Domagala-Kulawik, 2019).

1.2. Lung Adenocarcinoma

Primary lung adenocarcinoma is defined as a malignant epithelial neoplasm showing features of glandular differentiation. Its classification depends on the degree of glandular differentiation, as well as the degree of cytological atypia. Well-differentiated neoplasms are characterized by a proliferation of well-formed glands lined by atypical cells that infiltrate the surrounding stroma. On the other hand, poorly differentiated tumors grow as solid sheets of tumor cells with poorly formed glandular structures (Fletcher, 2013).

Within the lung adenocarcinoma there is a great variety of growth patterns including acinar, papillary, micropapillary, lepidic, solid and mucinous patterns (Cage, 2004). They are known to show significant morphological heterogeneity with various morphological characteristics and molecular abnormalities (Kumar, Abbas, & Aster, 2012).

The acinar pattern is characterized by invasive glands lined as the major component of the tumor. These glands have different sizes and shapes. Malignant cells that line the glands can be oval, cuboidal, or columnar. Also, the cells or lumen of the glands may contain mucin (Cage, 2004).

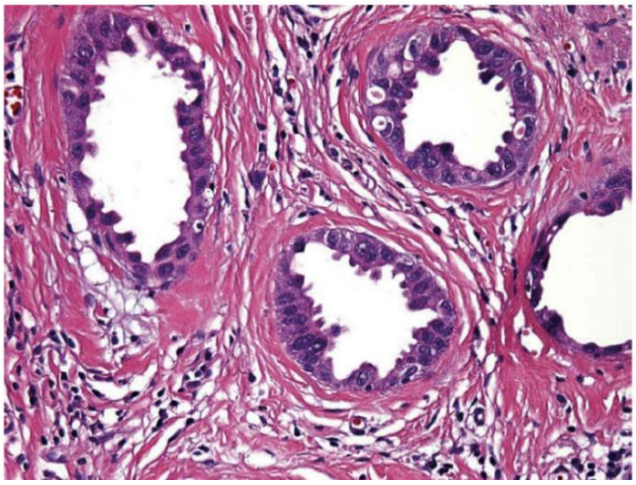

Figure 1. Acinar Adenocarcinoma with invasive glands (Cage, 2004).

In the papillary pattern, numerous papillary folds with thin stems of fibroconnective tissue are observed, completely filling and distorting the air spaces. In this pattern, malignant cells grow along the surface of the papillary fibrovascular cores in most of the tumor (Cage, 2004).

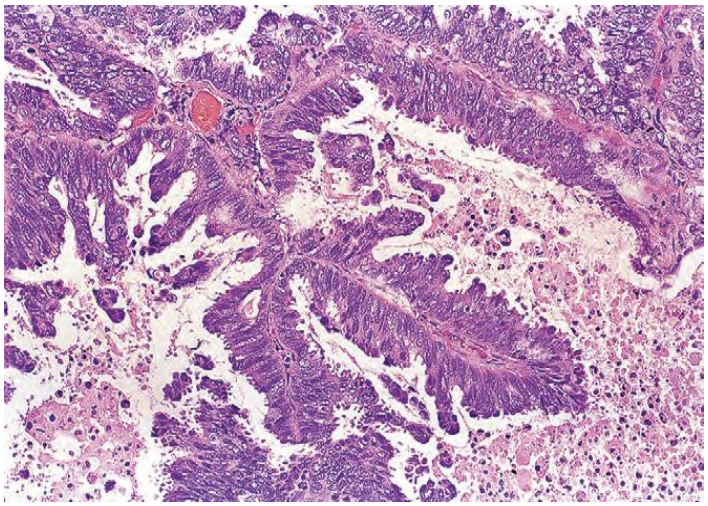

Figure 2. Papillary adenocarcinoma (Cage, 2004).

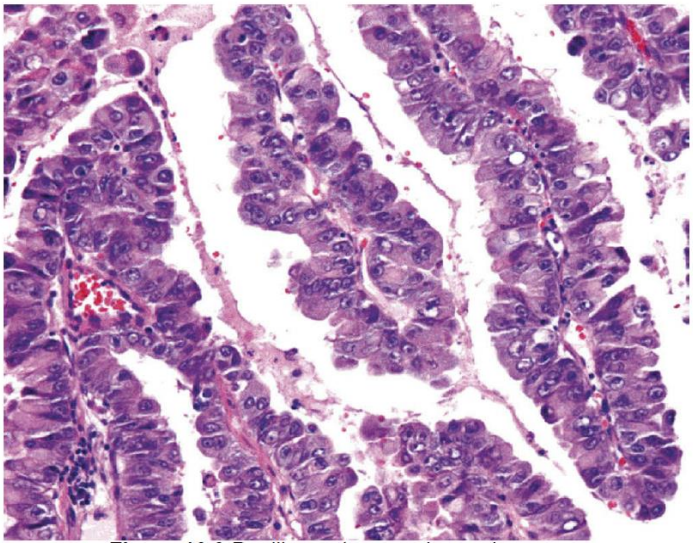

Figure 3. Papillary adenocarcinoma with fibrovascular cores and malignant cells on the surface (Cage, 2004).

On the other hand, the micropapillary pattern is a subtype of invasive adenocarcinoma, in which the majority of the tumor is composed of small

cuboidal malignant cells arranged in papillary tufts or folds without fibrovascular cores. Micropapillary adenocarcinoma is associated with a worse prognosis than other adenocarcinoma subtypes (Cage, 2004).

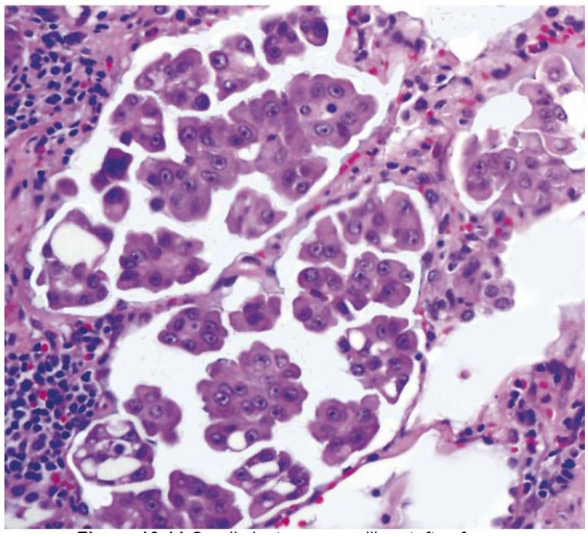

Figure 4. Micropapillary adenocarcinoma (Cage, 2004).

Lepidic carcinoma is characterized by a neoplastic proliferation of cells which grow exclusively along the lining of the alveolar walls, without invasion of the underlying septa or other structures. The cells are characterized by mild cellular atypia. In addition, they are able to present some mitotic activity (Cage, 2004).

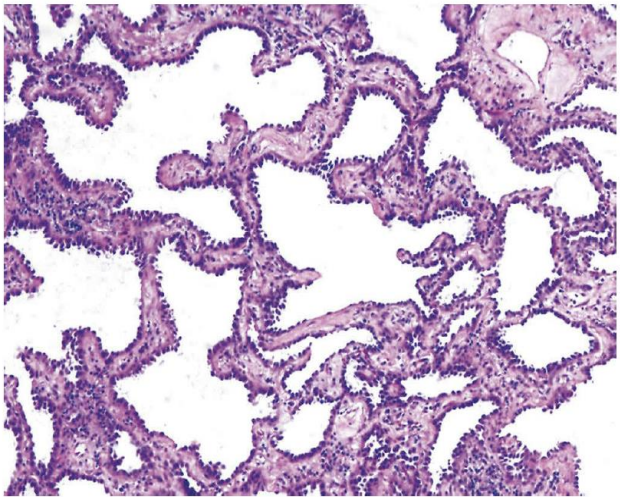

Figure 5. Lepidic carcinoma (Cage, 2004).

Solid adenocarcinomas are a subtype composed by solid sheets, or nests of polygonal malignant cells. Among the different subtypes of lung adenocarcinoma, those with a solid pattern seem to have a worse prognosis (Cage, 2004).

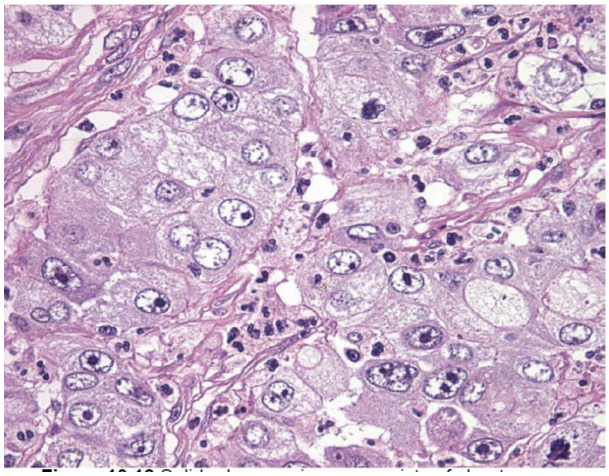

Figure 6. Solid adenocarcinoma with sheets of polygonal malignant cells (Cage, 2004).

Finally, the mucinous pattern is characterized by the accumulation of abundant mucin deposits, which destroys the normal lung parenchyma. The alveolar walls may show focally mucinous epithelium with atypia. Also, in this pattern, we can observe small groups of individually dispersed mucinous cells with mucin deposits.

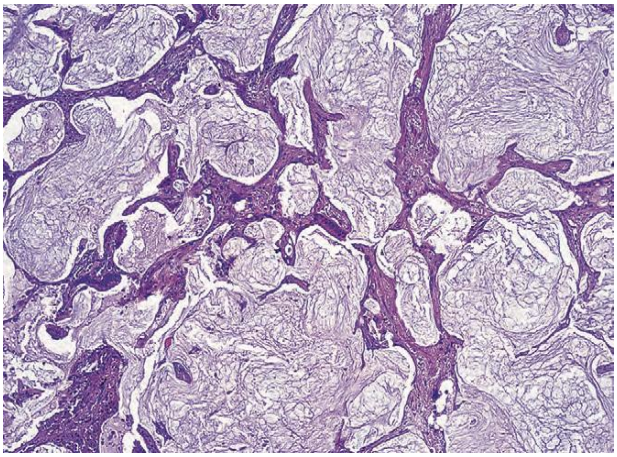

Figure 7. Mucinous adenocarcinoma (Cage, 2004).

Molecular pathology plays a fundamental role, since knowledge of the molecular biology of cancer has allowed not only to better understand the development of tumors, but also helps to predict sensitivity to chemotherapy and opens doors to the development of new more targeted therapeutic agents.

Adenocarcinomas often present gain-of-function mutations in growth factor receptor signaling pathways including receptor tyrosine kinases, such as EGFR, ALK, ROS, MET, and RET. In addition, they can also present mutations in the RAS genes, specifically in the KRAS isoform.

1.3. RAS

It is currently known that the alterations existing in the cellular genome affect the expression or function of certain genes responsible for controlling cell growth and differentiation. For this reason, they are considered the main cause of cancer. Much molecular research is focused on the study of genes that are altered in various tumor types in order to discover the role of these genes in carcinogenesis (Bos, 1989). Analyzing the different molecular pathways that underlie carcinogenesis, it should be borne in mind that the pathways do not act in isolation, they are interconnected with each other (Pecorino, 2012). One of the main signaling pathways and node of many other routes is the MAPK pathway. The kinases play a critical role in fundamental cell functions, such as cell progression, signal transduction and transcription. Therefore, they are important molecular targets for the design of anticancer drugs (Pecorino, 2012).

The MAPK pathway is one of the key mechanisms to transmit extracellular signals from the membrane to the intracellular compartments and to the nucleus through protein phosphorylation. In this pathway there are two groups of enzymes involved, mitogen-activated protein kinases (MAP)

and threonine-tyrosine dual-specificity phosphatases also known as MAPK phosphatases (MPKs). These enzymes have opposite roles coordinating to confer adequate signaling. Mitogen-activated protein kinases transduce environmental and developmental signals into adaptive, and programmed responses such as survival, proliferation, differentiation, inflammation, and apoptosis (Badve & Kumar, 2019). Within the MAPK pathway we find genes such as RAS, RAF or MEK. Multiple investigations focused on this pathway have led to the development of new and more specific therapies with greater efficacy and fewer side effects. Currently, there are already targeted therapies against some of the mutated genes, such as the case of tyrosine kinase inhibitors (TKI) for lung adenocarcinoma (Domagala-Kulawik, 2019).

One of the genes belonging to the MAPK pathway and frequently mutated in many tumor types are the RAS family genes, which are mutated in more than 50% of certain types of cancer. Within the Ras gene there are three isoforms, H-ras, N-ras and K-ras, being K-ras the most frequently mutated oncogene in cancer (Bos, 1989) (Kumar, Abbas, & Aster, 2012).

Ras works as a binary switch binding GDP in its inactive state, and GTP in its active mode. An inactive Ras protein that binds to GDP is stimulated by a guanine nucleotide exchange factor (GEF) to release its GDP and acquire a GTP molecule, thereby placing Ras in its active configuration. This signaling is stopped by Ras's intrinsic GTPase action, by which GTP is hydrolyzed to GDP (Drosten, Lechuga, & Barbacid, 2014).

Point oncogenic mutations caused by amino acid substitutions block this cycle by inactivating the intrinsic activity of GTPase, causing Ras to remain activated (Kumar, Abbas, & Aster, 2012). All Ras oncoproteins carry amino acid substitutions at residue 12, or less frequently at residues 13 and 61

(Weinberg, 2014). Residues 12 and 61 structurally show a close association with GTP γ-phosphate (Figure 8), that is why the substitutions of these residues reduce or eliminate GTPase activity and with it the ability to convert GTP to GDP by eliminating γ-phosphate (Weinberg, 2014).

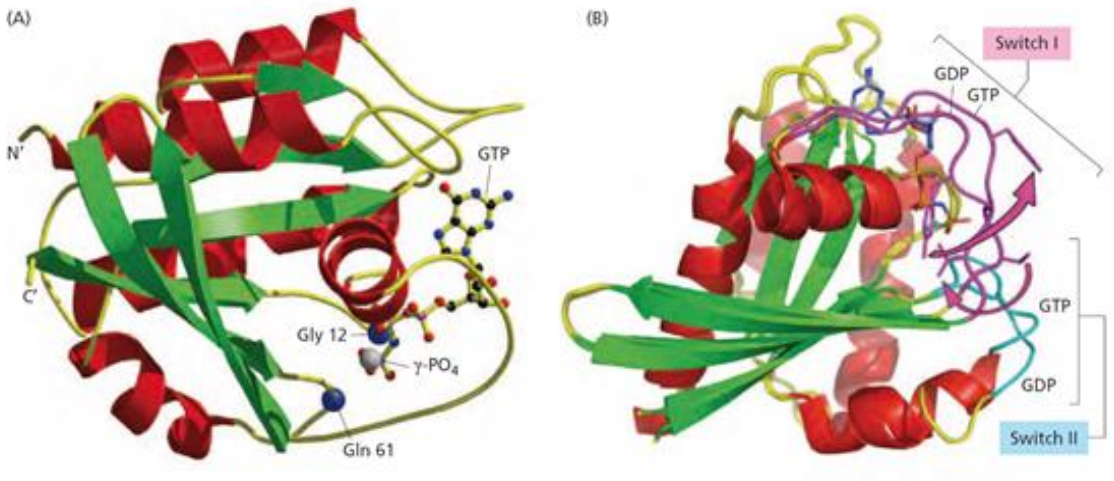

Figure 8. X-ray crystallography diagram, of the structure of the Ras protein, and its response to GTP binding (Canon, et al., 2019).

NRAS is predominantly mutated in melanoma and hematological malignancies, while HRAS are found in salivary gland and urinary tract cancers. The most frequently mutated member of the family is KRAS, with mutation rates of 86 to 96% in pancreatic cancers, 40 to 54% in colorectal cancers and 27 to 39% in lung adenocarcinomas (Kessler, et al., 2019). Within this oncogene KRAS G12C mutation is present in 13% of lung adenocarcinomas, 3% of colorectal cancers, and 2% of other solid tumors. Ras was the first oncogene discovered in human cancer, however, no therapeutic agent specifically directed to RAS has been approved for clinical use (Bar-Sagi, Knelson, & Sequist, 2020).

In lung cancer, KRAS gene mutations occur in 18–32% of adenocarcinomas, 12.8% of large cell carcinomas, 10% of adeno-squamous

carcinomas, and 1.6–7.1% of squamous cell carcinomas in Caucasian patients. Regarding lung adenocarcinoma, the G12C mutation is the most frequent alteration representing 52% of all KRAS mutations. Following in frequency, G12V mutations can be found in 11.6% of cases, G12D in 7.2% of cases, G12A appears in 2.9% of cases and G12S in 1.5% (Calvayra, Pradines, Pons, Mazières, & Guibert, 2016).

Recent studies seem to show a new opportunity for those patients with adenocarcinoma who present the G12C mutation. After decades of studies focused on the development of a drug for RAS mutated patients, AMGEN have developed a KRAS G12C inhibitor. In their study, they reveal that the inhibitor AMG510 binds to the oncoprotein and prevents its participation in tumor formation, thus reducing the size of the tumors. The researchers made a first evaluation in mice, in which they could observe a reduction in the size of the tumor and even the disappearance of it. After this, they carried out the same study with lung cancer patients, obtaining a reduction in tumor size of 34 to 67% in two patients. AMG510 seems to open new doors to targeted therapy in lung adenocarcinoma, although future trials are still needed. Given the frequency of KRAS mutations in lung adenocarcinoma, specifically the G12C mutation, incorporating the study of KRAS in clinical practice seems to be necessary since the development of inhibitors such as AMG510 would be an opportunity for those patients who they were not receiving effective treatment (Canon, et al., 2019).

2. HYPOTHESIS AND OBJECTIVES

2.1. Hypothesis

- Approximately 30% of patients will present a mutation at Gly12 (G12X).
- About half of the G12X mutations will be G12C, and may benefit from future treatment with KRAS G12C inhibitors.
- KRAS mutations do not coexist with EGFR, ALK, ROS1 and BRAF mutations. This fact will make it possible to optimize the panel for molecular categorization.
- There might be a relationship between the KRAS mutation at codon 12 and the morphological characteristics of the tumor.

2.2. Objectives:

- Establish the incidence of the G12C mutation in the lung adenocarcinoma study cohort.
- Optimization of the molecular panel in the categorization of pulmonary ADC.
- Histological correlation with molecular findings.

3. MATERIAL AND METHODS

3.1. Samples

This study includes 300 consecutive cases of stage IIb-IV lung adenocarcinoma diagnosed in the Department of Pathology, Hospital Universitario de Canarias. These tumors had been previously genotyped for the mutations included in the current guidelines for molecular diagnosis of lung cancer such as EGFR, ALK, and ROS1.

The DNA was stored after a manual dissection of adenocarcinoma areas, with a code number that does not identify the patient. For the purpose of this study, only coded samples were used, together with age and gender of the patient and no attempt was made to correlate the findings with the identity of the patients, which remained confidential in their protected electronic clinical history.

3.2. DNA purification

DNA purification takes place on two consecutive days.

- **First day:**

Recent blocks are selected with tissue that has not spent more than 72hrs in formalin. Once selected, 8 µm sections are made.

In those cases, in which the block has a majority of tumors and the non-tumor tissue can be removed from the block itself, the cutting tape is taken, that is, 2 8-µm cuts directly from the microtome with tweezers and inserted into a 1.5 ml Eppendorf. To remove the paraffin, we add 1 ml of xylene at 56ºC for 5 minutes, centrifuge and aspirate the xylene. After this, 1 ml of Ethanol is added and after 5 minutes the ethanol is centrifuged and aspirated. The remains are allowed to evaporate in the thermoblock with the lid open.

For very small tissue samples, the desired fragment is extracted with a needle and inserted into a 1.5 ml Eppendorf tube to continue with the same steps as in the previous case.

Finally, in those samples that need macrodissection on the slides, to select only the neoplastic area, the sample is deparaffinized and hydrated. To do this, we start with 2 washes with Xilol for 5 minutes each, followed by a 100% ethanol wash for 30 seconds, a 96% Ethanol wash for 30 seconds, and

another 30-second wash of 90% ethanol. Tubes are labeled with the sample number and 400 µl TENS or 180 µl lysis buffer (Roche) and 40 µl of proteinase K at 10 mg/ml are added. The tumor area is selected and labeled on an identical slide but stained with Hematoxylin-Eosin, with a beveled disposable tip moistened in the TENS + proteinase K solution previously prepared, the tissue to be purified is moistened and collected in the previously marked 1.7ml microfuge tube.

All tubes are incubated at 56 ° C overnight.

- **Second day:**

We start with an inactivation in the thermoblock at 90 ° C for one hour. After this, two sets of tubes are labeled with the sample number. The first set has 500 µl of Phenol-Chloroform and the second one 40 µl of AcNa.

The previously inactivated tubes are centrifuged for 2 minutes at maximum rpm and the supernatant is decanted in the corresponding phenol-chloroform tube. The tubes are shaken for one minute to mix the phenol solution and the lysate, then centrifuged the at maximum (13000 rpm) for 5 minutes.

After centrifugation, the aqueous phase is passed using a Pasteur pipette to the tube with corresponding AcNa taking care not to add the interface. Add 100% Ethanol to each tube to fill it up and shake by hand again until the solution is well mixed. Once mixed it is left for 1 hour at -20ºC in the freezer.

After one hour, the tubes are centrifuged for 15 minutes at maximum speed, the supernatant is removed and 500 µl of 70% Ethanol is added. It is centrifuged again for 5 minutes at maximum speed and the supernatant is removed again and the remaining Ethanol is allowed to evaporate in the

thermoblock with the lid open. Finally, the pellet is resuspended in 50 µl of TE.

Once the DNA was purified, it was quantified using the Nanodrop. For this, 1 µl of H20 is first added and quantified as blank. After this, the sample is quantified by adding 1 µl of it. (following NanoDrop user guide).

3.3. PCR

In order to carry out sequencing by pyrosequencing, it is necessary to previously perform PCR on the different samples. PCR is a basic, almost ubiquitous technique that provides sensitivity and specificity to the analysis. This technique allows us to make numerous copies after between 30 and 40 cycles with three stages each to later be able to analyze the amplification products.

Therascreen KRAS Pyro kit was used for PCR. It is a molecular detection kit for the identification of mutations and deletions in the KRAS gene. The kit contains primers and reagents for the amplification of the KRAS gene, buffers, primers and reagents for the detection and quantification of mutations in real time using Pyrosequencing technology in the PyroMark Q24 system.

First, a reaction mixture is prepared from the kit reagents following the instructions below.

Reagent	Volume/reaction (µl)
PyroMark PCR 2x Master Mix	12.5
Coraload 10x reagent	2.5
Primer	1.0
Water	4.0
Total volume	20

Table 1. Reagents and volumes per sample needed for a PCR reaction.

For ease of pipetting, a MasterMix is prepared in one tube approximately every 20 samples. This mix contains 180 µl of PyroMark PCR 2x Master Mix, 120 µl of water and 37.5 µl of Coral1oad 10x. For each sample, add 15 µl of the prepared mixture and 0.5 µl of the first mixture and mix well. After this, about 50 ng of the sample to be analyzed are added. As each sample is at a different concentration previously measured with the NanoDrop we follow the following table.

Concentration (ng/ µl)	Sample volume (µl)
< 24	2
24-100	1
>100	Dilute with water

Table 2. DNA volume required for the PCR reaction based on the DNA sample concentration.

Once the samples have been added, the tubes are sealed with adhesive tape and taken to the previously programmed thermocycler with an optimized cycling protocol.

			Comments
Initial activation step:	15 minutes	95°C	HotStarTaq DNA polymerase is activated by this heating step.
3-step cycling:			
Denaturation	20 seconds	95°C	
Annealing	30 seconds	53°C	
Extension	20 seconds	72°C	
Number of cycles	42		
Final extension:	5 minutes	72°C	

Table 3. Cycling protocol for the PCR reaction (Qiagen, 2015)

3.4. Pyrosequencing

For the genotyping of the tumor, the KRAS pyrosequencing kit (Qiagen) was used. The therascreen KRAS Pyro Kit is an in vitro nucleic acid sequence detection test that uses pyrosequencing technology for the quantitative detection of mutations in codons 12, 13 and 61 of the KRAS gene in genomic DNA obtained from human tissue samples (Qiagen, 2015).

The region of interest is amplified by PCR technique and then the defined region is sequenced. The adjacent sequences of the defined positions are used as normalization and reference peaks for quantification and quality assessment of the analysis (Qiagen, 2015).

After PCR is performed with primers targeting codons 12/13, the amplicons are immobilized on Streptavidin Sepharose® High Performance beads. Single-stranded DNA is prepared, and the corresponding sequencing primers anneal to the DNA. Samples are analyzed on the PyroMark Q24 system using a run setup file and a run file (Qiagen, 2015).

In addition, unmethylated control DNA is included as a positive control for PCR and sequencing reactions, necessary to make a correct result interpretation.

Table 6. Master mix for DNA immobilization

Component	Volume/sample (µl)
Streptavidin Sepharose High Performance	2
PyroMark Binding Buffer	40
Water (H_2O, supplied)	28
Total volume	**70**

Table 4. Master mix for DNA immobilization. (Qiagen, 2015)

This mixture is added to the PCR product and stirred 5-10 minutes at 1,400 rpm.

Next, 0.7 µl of KRAS 12 / 13 sequencing primer is diluted in 25 µl of annealing PyroMark buffer per sample on a PyroMark Q24 plate (Qiagen, 2015).

The PCR product is taken to the workstation. Filter probes of the vacuum tool are introduced in order to capture the microspheres that contain the immobilized template. The vacuum tool is transferred to the container containing 40 ml of 70% ethanol, followed by another container with 40 ml of denaturation solution and finally by another 40 ml of washing solution (Qiagen, 2015).

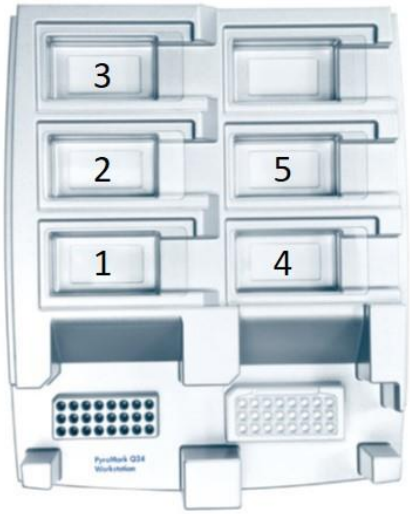

Figure 9 and 10. Work station for pyrosequencing. (Qiagen, 2020)

Once the liquid is drained and the vacuum is disconnected, the microspheres are released in the PyroMark Q24 plate by lowering the filter probes into the previously prepared mixture with the sequencing primer diluted in the annealing buffer and gently moving it side to side.

The PyroMark Q24 plate with samples are plated at 80 ° C for two minutes using the PyroMark Q24 preheated plate holder. After the two minutes have elapsed the PyroMark Q24 plate is removed from the hot plate holder and placed on the second holder that had been left at room temperature for 10-15 minutes to allow the samples to cool to room temperature (Qiagen, 2015).

During the 15 minutes, the analytical series to be performed is configured to be able to observe the volume of the nucleotides, enzyme and substrate necessary for each series (Qiagen, 2015).

In the PyroMark Q24 cartridge, always with the front label, the necessary reagents are placed according to the number of samples following the following scheme:

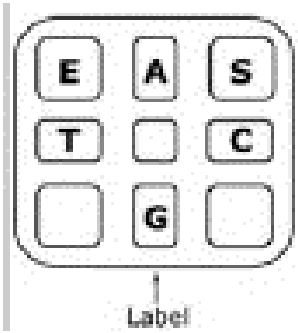

Figure 11. Scheme of the cartridge for pyrosequencing. E= enzyme; S= substrate; A=Adenine; C= Citosine; G=Guanine; T=Timine (Qiagen, 2015).

Once the cartridge is prepared and after 15 minutes the cartridge is placed in its compartment and the plate in the plate rack. After this, the USB in which the analytical series file has previously been saved is connected and "Run" is started (Qiagen, 2015).

Figure 12 and 13. Robot for pyrosequencing (Qiagen, 2020).

When the analytical series ends, the results will be saved on the USB and will be accessible on the computer.

For each sample we observe the results on a pyrogram. Comparing with the control DNA pyrogram ("GGT" at codon 12) we can analyze possible mutations in each case (Qiagen, 2015).

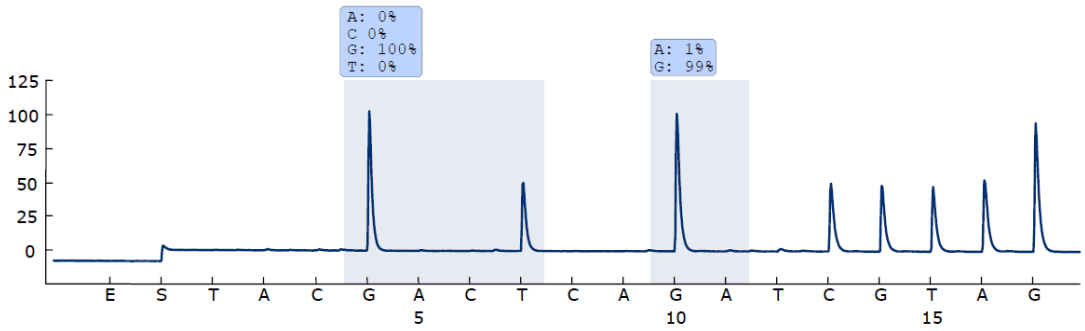

Figure 14. Control DNA pyrogram (Qiagen, 2015).

Mutations at codon 12 or 13 can be analyzed thanks to the pyrogram, observing a variation in relation to the control pyrogram (Qiagen, 2015).

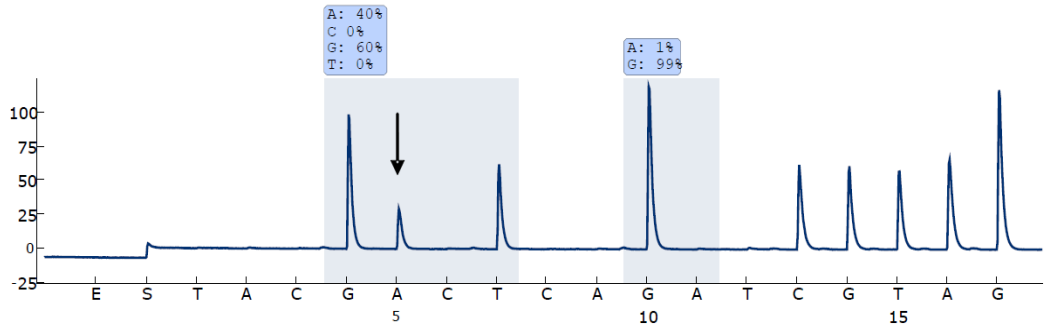

Figure 15. Pyrogram with a G12D mutation (GTT>GAT) (Qiagen, 2015).

In the G12C mutation, the variation is observed outside the main study area, therefore the program will show an alert (yellow or red box) (Qiagen, 2015).

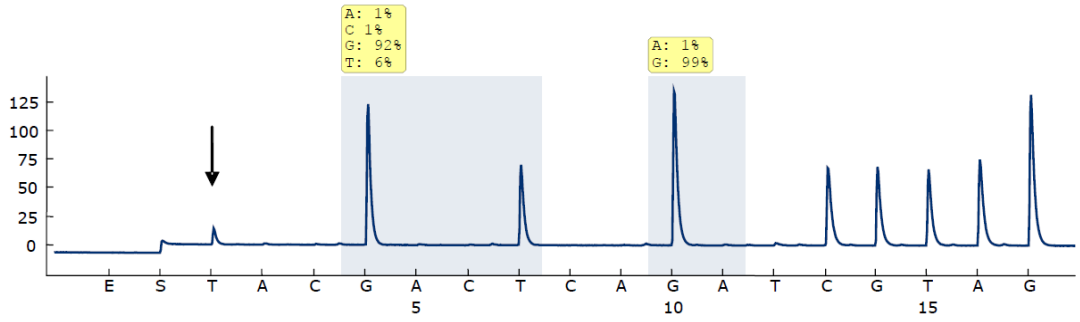

Figure 16. Pyrogram of a G12C mutation (Qiagen, 2015).

To analyze this mutation, the analyzing sequence should be modified. It is modified from GNTGRCGTAGG to NGTGRCGTAGGC in order to detect base 2 of codon 12 (nucleotide 35) (Qiagen, 2015).

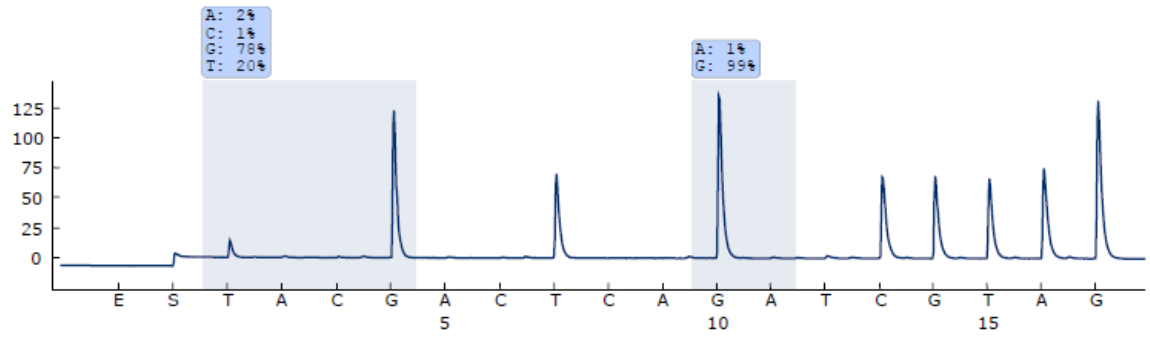

Figure 17. G12C pyrogram after the reanalysis of the sample (Qiagen, 2015).

1.1. Statistical Analysis

The evaluation of the different mutations was performed after recording all the results. Cross tabulation was performed to observe the possible coexistence of mutations. A chi-square test was used for comparing two qualitative variables. All data processing for statistical analysis was performed with IBM SPSS software (version 25.0 for Windows).

4. RESULTS.

Of the 300 patients studied, KRAS was mutated in 34.88% of the cases being KRAS G12C the most frequent mutation (15.6%; Graph 1 and Table 5).

Eight KRAS mutated adenocarcinomas (7.76%; Table 13) also carried EGFR mutations (exon 19 deletion, n = 1; L858R mutation, n = 7), and in two others (1.94%; Table 16) the KRAS G12C mutation coexisted with BRAF V600E. None was associated to either ALK translocations.

We did not find statistically significant association between histology subtypes of lung adenocarcinoma and mutations in KRAS, not even the mucinous phenotype, which has been suggested to harbor KRAS mutations in a higher proportion (p = 0.318; Table 18).

4.1. KRAS mutation.

KRAS mutation was studied in 301 patients, 196 of them had no mutations in codons 12/13 of KRAS (34.88%), while 105 (65.12%) had some mutation in KRAS (Graph 1 and Table 5).

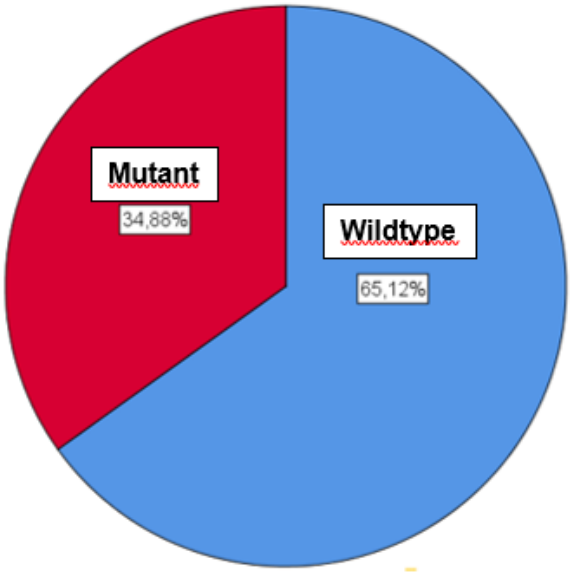

Graph 1. Pie chart representing the different KRAS frequencies.

KRAS

	Frequency	Percentage	Valid Percentage	Accumulated Percentage
Wildtype	196	65,1	65,1	65,1
Mutant	105	34,9	34,9	100,0
Total	301	100,0	100,0	

Table 5. Frequency study of KRAS mutations.

Among the missense mutations in KRAS, there are different frequent alleles, replacing glycine 12 or 13 by another amino acid. Within the 301 sequenced cases, the most frequent G12C mutation appeared in 15.61% of the cases (47 patients); the second most frequent changes were G12V (8.6%), followed by G12A (4.32%) (Graph 2 and Table 6).

Other mutations found in our series include G12D (3.65%), G12R (0.7%), G12S (0.3%) and G13 (1.33%) (Graph 2 and Table 6).

	Frequency	Percentage	Valid Percentage	Accumulated Percentage
G12A	13	4,3	4,3	4,3
G12C	47	15,6	15,6	19,9
G12D	11	3,7	3,7	23,6
G12R	2	,7	,7	24,3
G12S	1	,3	,3	24,6
G12V	26	8,6	8,6	33,2
G13	4	1,3	1,3	34,6
Wildtype	197	65,4	65,4	100,0
Total	301	100,0	100,0	

Table 6. Frequency study of the different KRAS mutations.

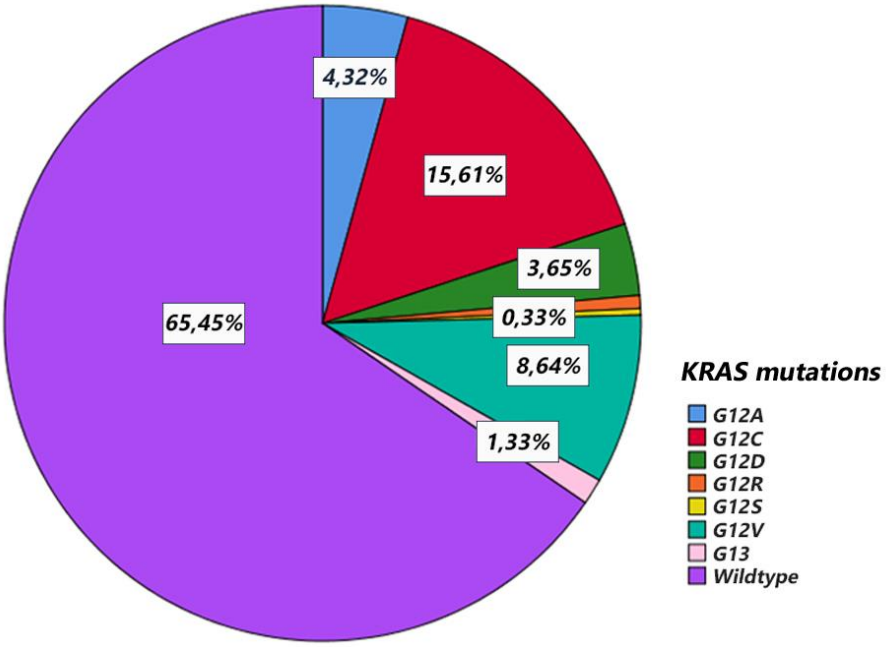

Graph 2. Pie chart representing the frequencies of the different KRAS mutations.

In the KRAS study, an age and gender analysis was also carried out in order to determine the most frequent age range as well as the most frequent gender to find this mutation.

21% of KRAS mutated patients are between 60 and 64 years old. The second most frequent age range is between 55 and 59 years (18.5%; Table 5).

		KRAS		
		Wildtyppe	Mutant	Total
Age	35-39	1	0	1
	40-44	1	0	1
	45-49	4	5	9
	50-54	6	7	13
	55-59	13	15	28
	60-64	29	17	46
	65-69	27	12	39
	70-74	35	11	46
	75-79	23	7	30
	80-84	7	5	12
	85-89	8	2	10
	90-94	2	0	2
Total		156	81	237

Table 7. Cross tabulation Age by range * KRAS mutation to know the KRAS cases according to the age. Frequency of mutant cases: **45-49:** 5/81=6.71%; **50-54:** 7/81=8.64%; **55-59:** 15/81=18.52%; **60-64:** 17/81=20.99%; **65-69:** 12/81=14.81%; **70-74:** 11/81=13.58%; **75-79:** 7/81=8.65%; **80-84:** 5/81= 6.17%; **85-89:** 2/81=2.47%.

However, the KRAS G12C mutation was found more frequently in the previous age range, between 55 and 59 years.

For the relation between sex and mutation in KRAS, 280 results were analyzed.

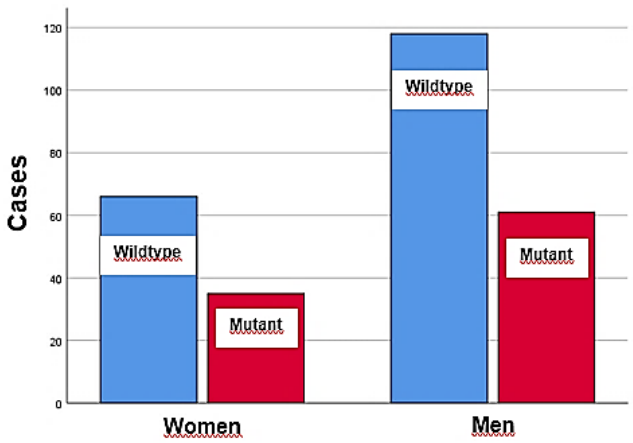

Graph 3. Histogram representing the classification on KRAS according to the gender.

		KRAS		
		Wildtype	Mutant	Total
Sex	Women	66	35	101
	Men	118	61	179
Total		184	96	280

Table 8. Cross tabulation Sex * KRAS to know the cases of KRAS according to gender.

In men, 61 of 179 present a mutation in KRAS (34.08%) In the case of women, 35 of 101 cases present this mutation (34.65%) (Graph 3 and Table 8).

4.2. EGFR mutation

Within 301 cases analyzed, 293 had a previous study of EGFR. Of these 293 cases, 52 presented the EGFR mutation, which is 17.7% (Graph 4 and Table 9).

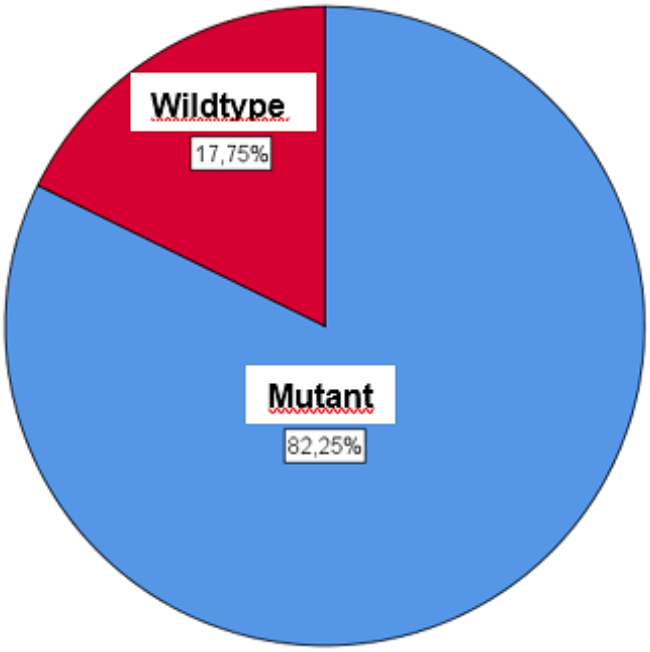

Graph 4. Pie chart representing the different EGFR frequencies

EGFR				
	Frequency	Percentage	Valid percentage	Accumulated Percentage
Wildtype	241	82,3	82,3	82,3
Mutant	52	17,7	17,7	100,0
Total	293	100,0	100,0	

Table 9. Frequency study of EGFR mutations.

As in KRAS, a study of age and sex was also carried out in EGFR to determine the most frequent age range and the most frequent sex in this mutation.

22'86% of EGFR mutated patients are between 70 and 74 years old. 20% of the mutated patients have an age in the range 65-69 (Table 10).

		EGFR		
		Wildtype	Mutant	Total
Age	35-39	1	0	1
	40-44	1	0	1
	45-49	9	0	9
	50-54	11	2	13
	55-59	27	1	28
	60-64	38	6	44
	65-69	32	7	39
	70-74	37	8	45
	75-79	24	6	30
	80-84	8	4	12
	85-89	9	1	10
	90-94	2	0	2
Total		199	35	234

Table 10. Cross Tabulation Age by range * EGFR cases to know the EGFR cases according to the age. Frequency of mutant cases: **50-54:** 2/35=5.71%; **55-59:** 1/35=2.86%; **60-64:** 6/35=17.14%; **65-69:** 7/35=20.00%; **70-74:** 8/35=22.86%; **75-79:** 6/35=17.14%; **80-84:** 4/35= 11.42%; 85-89: 1/35=2.86%.

Regarding sex, 29 out of 100 women presented a mutation in EGFR (29%) while only 16 men out of 174 men presented the same mutation (9.19%).

The EGFR mutation seems to be more frequent in women than in men.

4.3. ALK mutation

Among the 301 patients analyzed, 274 had a previous study of the ALK mutation, of which only 6 had an ALK mutation (2.2%; Graph 5 and Table 11).

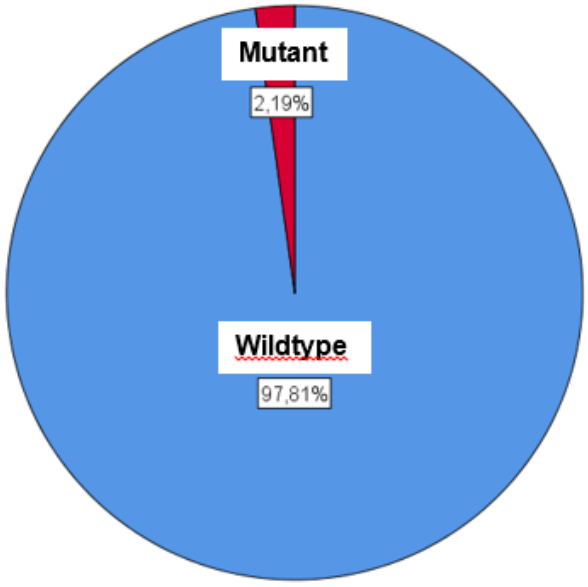

Graph 5. Pie chart representing the different ALK frequencies

ALK

	Frequency	Percentage	Valid Percentage	Acumulated percentage
Wildtype	268	97,8	97,8	97,8
Mutant	6	2,2	2,2	100,0
Total	274	100,0	100,0	

Table 11. Frequency study of ALK mutations.

4.4. BRAF mutation

Among the 301 patients analyzed, 274 had performed a previous study of the BRAF mutation, of which only 4 had a BRAF mutation (1.5%; Graph 6 and Table 12).

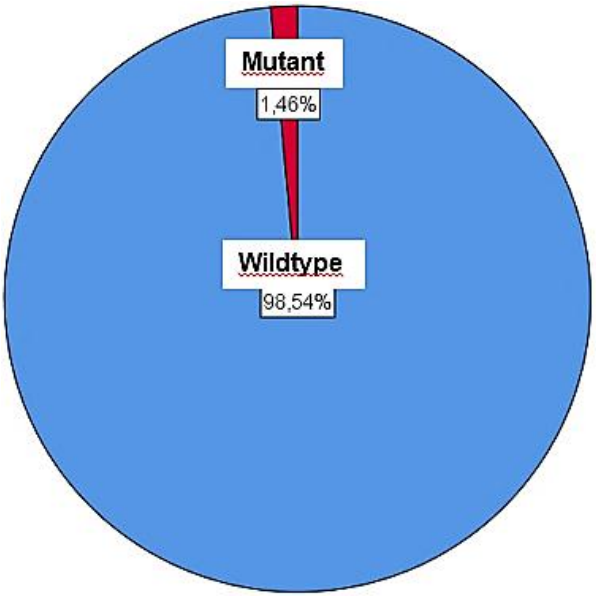

Graph 6. Pie chart representing the different BRAF frequencies.

BRAF	Frequency	Percentage	Valid percentage	Accumulated percentage
Wildtype	270	98,5	98,5	98,5
Mutant	4	1,5	1,5	100,0
Total	274	100,0	100,0	

Table 12. Frequency study of BRAF mutations.

4.5. Coexistence of mutations

4.5.1. EGFR AND KRAS

The coexistence study of KRAS and EGFR mutations was performed in 293 cases. Eight of the 52 EGFR mutated patients also had a KRAS

mutation. Specifically, 1 of the patients presented a deletion of exon 19 in EGFR and another 7 presented the L858R mutation (Table 13).

		KRAS		
		Wildtype	Mutant	Total
EGFR	Wildtype	146	95	241
	Mutant	44	8	52
Total		190	103	293

Table 13. Cross tabulation KRAS * EGFR to study the coexistence of both mutations.

Within the different KRAS mutations, the highest coexistence with EGFR was found in the G12C mutation (4 patients), followed by the G12D mutation (2 patients) (Table 14).

		KRAS								Total
		G12A	G12C	G12D	G12V	G12R	G12A	G13	Wildtype	
EGFR	Wildtype	12	43	8	2	1	25	4	146	241
	Mutant	1	4	2	0	0	0	0	45	52
Total		13	47	10	2	1	25	4	191	293

Table 14. Cross tabulation KRASmutations * EGFR to study the coexistence of EGFR with the different KRAS mutations.

4.5.2. ALK AND KRAS

The coexistence study of KRAS and ALK mutations was performed in 274 cases. Of the 6 patients with an ALK mutation, none presented KRAS mutation (Table 15).

		KRAS		
		Wildtype	Mutant	Total
ALK	Wildtype	169	99	268
	Mutant	6	0	6
Total		175	99	274

Table 15. Cross tabulation KRAS* ALK to study the coexistence of both mutations.

4.5.3. BRAF AND KRAS

Of the 4 cases that with a BRAF mutation, 2 also had a KRAS mutation (50%; Table 16). However, this coexistence did not occur with a G12C mutation.

		KRAS		
		Wildtype	Mutant	Total
BRAF	Wildtype	173	97	270
	Mutant	2	2	4
Total		175	99	274

Table 16. Cross tabulation KRAS* BRAF to study the coexistence of both mutations.

4.6. Morphological correlation

This study included a correlation between different histological patterns and the presence of KRAS mutation.

8 patients presented a mucinous pattern, of which 4 also had mutations in KRAS (Table 17).

		KRAS		
		Wildtype	Mutant	Total
Mucinous pattern	No	134	66	200
	Yes	4	4	8
Total		138	70	208

Table 17. Cross tabulation KRAS* mucinous pattern to study the frequency of KRAS in the mucinous pattern.

The chi-square test revealed a p-value of 0.318, and the Null Hypothesis could not be rejected, therefore there is no significant correlation between the mucinous morphological pattern and the KRAS mutation (Table 18).

Chi-square test

	Value	df	Asymptotic Significance (2-sided)	Exact Sig. (2-sided)	Exact Sig (1-sided)
Pearson´s Chi-Square	,996[a]	1	,318		
Continuity correction[b]	,380	1	,538		
Likelihood Ratio	,943	1	,332		
Fisher´s Exact Test				,447	,262
Linear-by-Linear Association	,991	1	,320		
N of Valid Cases	208				

a. 1 cells (25,0%) have expected count less than 5. The minimum expected count is 2,69.

b. Computed only for a 2x2 table.

Table 18. Chi-square test to study the relation between the mucinous pattern and the KRAS mutation.

Of the 104 patients with a solid pattern, 39 had a KRAS mutation (37.5%; Table 19).

		KRAS		
		Wildtype	Mutant	Total
Solid pattern	No	75	32	107
	Yes	65	39	104
Total		140	71	211

Table 19. Cross tabulation KRAS* solid pattern to study the frequency of KRAS in the solid pattern.

The p-value obtained is 0.332, therefore, we cannot reject the null hypothesis. There is no significant correlation between the solid pattern and the presence of mutations in KRAS (Table 20).

Chi-square test

	Value	df	Asymptotic Significance (2-sided)	Exact Sig. (2-sided)	Exact Sig (1-sided)
Pearson´s Chi-Square	,940[a]	1	,332		
Continuity correction[b]	,681	1	,409		
Likelihood Ratio	,940	1	,332		
Fisher´s Exact Test				,387	,205
Linear-by-Linear Association	,935	1	,333		
N of Valid Cases	213				

a. 0 cells (0,0%) have expected count less than 5. The minimum expected count is 35,64.

b. Computed only for a 2x2 table.

Table 20. Chi-square test to establish the possible relation between the solid pattern and the KRAS mutation.

The acinar pattern was observed in 115 patients of which 39 had a KRAS mutation (33.91%; Table 21).

		KRAS		
		Wildtype	Mutant	Total
Acinar pattern	No	63	31	94
	Yes	76	39	115
Total		139	70	209

Table 21. Cross tabulation KRAS* acinar pattern to study the frequency of KRAS in the acinar pattern.

Despite the high percentage, there does not seem to be a significant histological correlation.

Chi-square test

	Value	df	Asymptotic Significance (2-sided)	Exact Sig. (2-sided)	Exact Sig (1-sided)
Pearson´s Chi-Square	,020[a]	1	,887		
Continuity correction[b]	,000	1	1,000		
Likelihood Ratio	,020	1	,887		
Fisher´s Exact Test				1,000	,503
Linear-by-Linear Association	,020	1	,887		
N of Valid Cases	209				

a. 0 cells (0,0%) have expected count less than 5. The minimum expected count is 31,48.

b. Computed only for a 2x2 table.

Table 22. Chi-square test to study the possible relation between the acinar pattern and the KRAS mutation.

A p-value of 0.887 was obtained, so there is insufficient evidence to reject the null hypothesis, so there is no significant relationship between the acinar pattern and the presence of a mutation in KRAS (Table 22).

On the other hand, 18 patients presented a papillary pattern, of which 5 were KRAS mutants (27.77%; Table 23).

		KRAS		
		Wildtype	Mutant	Total
Papilar pattern	No	126	65	191
	Yes	13	5	18
Total		139	70	209

Table 23. Cross tabulation KRAS* papillary pattern to study the frequency of KRAS in the papillary pattern.

Chi-Square test

	Value	df	Asymptotic Significance (2-sided)	Exact Sig. (2-sided)	Exact Sig (1-sided)
Pearson´s Chi-Square	,582[a]	1	,445		
Continuity correction[b]	,399	1	,527		
Likelihood Ratio	,578	1	,447		
Fisher´s Exact Test				,512	,263
Linear-by-Linear Association	,580	1	,446		
N of Valid Cases	301				

a. 0 cells (0,0%) have expected count less than 5. The minimum expected count is 32,09.

b. Computed only for a 2x2 table.

Table 24. Chi-square test to analyze the possible relation between the papillary pattern and the KRAS mutation.

The p-value obtained is 0.445, therefore, we cannot reject the null hypothesis. There is no significant correlation between the papillary pattern and the presence of mutations in KRAS (Table 24).

The lepidic pattern was observed in 26 of the analyzed patients. Of the 26 patients, 8 had a KRAS mutation (30.76%; Table 25).

		KRAS		
		Wildtype	Mutant	Total
Lepidic pattern	No	118	61	179
	Yes	18	8	26
Total		136	69	205

Table 25. Cross tabulation KRAS* lepidic pattern to study the frequency of KRAS in the lepidic pattern.

As in the other histological patterns, in this type of pattern there is also no significant relationship with the presence of mutations in KRAS (p-value = 0.753; Table 26).

Chi-Square test

	Value	df	Asymptotic Significance (2-sided)	Exact Sig. (2-sided)	Exact Sig (1-sided)
Pearson´s Chi-Square	,099[a]	1	,753		
Continuity correction[b]	,009	1	,926		
Likelihood Ratio	,100	1	,751		
Fisher´s Exact Test				,827	,471
Linear-by-Linear Association	,099	1	,753		
N of Valid Cases	206				

a. 0 cells (0,0%) have expected count less than 5. The minimum expected count is 8,71.

b. Computed only for a 2x2 table.

Table 26. Chi-square test to study the possible relation between the lepidic pattern and the KRAS mutation.

Finally, the micropapillary pattern was observed only in 2 patients, of whom none had a KRAS mutation. As in the other histological patterns, there is no significant relationship between the micropapillary pattern and the KRAS mutation (p-value = 0.313; Table 27).

Chi-Square test

	Valor	df	Significación asintótica (bilateral)	Significación exacta (bilateral)	Significación exacta (unilateral)
Pearson´s Chi-Square	1,017[a]	1	,313		
Continuity correction[b]	,065	1	,798		
Likelihood Ratio	1,641	1	,200		
Fisher´s Exact Test				,552	,441
Linear-by-Linear Association	1,012	1	,314		
N of Valid Cases	209				

a. 2 cells (50,0%) have expected count less than 5. The minimum expected count is 8,71.

b. Computed only for a 2x2 table.

Table 27. Chi-square test to study the possible relation between the micropapillary pattern and the KRAS mutation.

5. DISCUSSION

Despite great advances in molecular biology, lung cancer remains a serious cancer problem worldwide. Over the years, thanks to the development of new targeted therapies that are more specific and less harmful to the patient, significant progress has been observed in achieving prolonged survival (Domagala-Kulawik, 2019).

Lung cancer has evolved a lot over the years, not only in the different treatment alternatives, also in its histological classification at the time of diagnosis.

Within lung cancer, adenocarcinoma seems to have an important weight, not only due to its severity and incidence, also because in recent years we have observed an increase of cases in non-smokers and never smokers. This fact makes it necessary to pay special attention to the search for a cause and possible treatment alternatives.

Previous epidemiological studies show that in the European population EGFR is mutated in about 15% of cases, including exon 19 deletion and L858R substitution as the most prevalent mutations. The results are similar to those obtained in this study (17.75%; Graph 4 and Table 9). Mutations in EGFR have been extensively studied because these common mutations are among a group of alleles that are known to be predictive biomarkers of good therapeutic response to treatments based on inhibitors of the thyrosine kinase activity of EGFR (EGFR-TKIs). EGFR-TKIs are available as first-line therapy, improving survival compared to standard platinum treatment (Garrido, Conde, & J de Castro, 2019). The presence of this targeted therapy makes the study of EGFR necessary, as indicated in molecular diagnostic guidelines.

ALK rearrangements according to previous epidemiological studies seem to occur in about 3% of cases. The same studies place these mutations in cases where neither EGFR nor KRAS mutations occur (Calvayra, Pradines, Pons, Mazières, & Guibert, 2016). Similar data (2.19%: Graph 5 and Table 11) were also obtained in our study and there was no coexistence of KRAS and ALK. As for EGFR, there are targeted inhibitor-based therapies for those patients with an ALK translocation, which must be carefully selected to avoid possible resistance.

Mutations in BRAF have been documented to appear in 2% of cases coinciding with our study, in which BRAF appears in 1.46% (Graph 6 and Table 12). Other studies affirm that a mutation in BRAF is mutually exclusive with other alterations present in the tumor, so there is no coexistence of BRAF with KRAS. However, in our study we have found such coexistence, so it would be necessary to delve more deeply in order to draw more exhaustive conclusions.

Due to the clinical benefit provided by targeted therapies in this disease, it is key to identify the possible molecular alterations of the different tumors.

Epidemiological studies of molecular biology of lung cancer, rank KRAS mutations as the most frequent mutation, which can be found in between 18 and 32 percent of the cases. However, the data obtained in this study even seems to exceed these figures (35%, Graph 1 and Table 5). For this reason, a therapeutic target for this gene is increasingly necessary. However, the great variety of mutations within this isoform, in which glycine at codon 12 is replaced by other amino acids (aspartic, valine, alanine, cysteine...), represents a formidable challenge to the development of targeted therapy. Thus, KRAS mutations are often described as an unfavorable biomarker in

patients with resected pulmonary adenocarcinoma. Furthermore, they do not seem to show significant improvements with specific treatments.

On the other hand, other clinically approved inhibitors for various MAPK proteins such as EGFR-TKI, MEK or BRAF inhibitors do not seem to show an optimal result either, they are even contraindicated for the treatment of KRAS mutant tumors. This is because KRAS mutations cause constant activation of signaling pathways regardless of EGFR action. Therefore, inhibiting EGFR will not stop mutant KRAS from activating signaling pathways.

A patient with pulmonary ADC and a KRAS mutation have a worse prognosis, and the lack of specific treatment reduces their survival.

Much research over the years has focused on trying to learn more and understand the KRAS way of action, which despite of being the first oncogene described it has always been a big question mark. Recent research based on structural studies using crystallography, have allowed us to better understand the structure of this isoform and its different mutations, thus advancing on the development of a possible treatment. The latest research has developed G12C-specific covalent inhibitors targeting mutated cysteine that appear to show promising data. AMGEN have developed a KRAS inhibitor that works by inhibiting the G12C mutation. This drug called AMG510 binds to the oncoprotein, preventing its participation in tumor formation causing a reduction in the size and even its disappearance.

Recent studies with this drug appear to provide some hope, as AMG510 is the first-class first KRAS (G12C) inhibitor with evidence of clinical activity in patients. With these studies AMG510 could be an effective antitumor agent. However, this is only the beginning, since KRAS presents

different mutations for which an inhibitor would also be an option to consider.

Considering the high percentage of patients with a KRAS mutation and the coexistence of mutations we should consider an option including a KRAS in a molecular panel for the categorization of pulmonary ADC. Furthermore, when AMG510 is clinically approved, 15% of patients could benefit from the new treatment, being necessary the molecular categorization of the tumor.

The fundamental histological observation for the diagnosis of the patient already provides ideas about the prognosis. Certain tumor growth patterns are known to be associated with a worse diagnosis. This fact makes us consider the idea that certain mutations are associated with different histological patterns. However, no relationship was found between the presence of the mutations and the histological pattern. Therefore, the histological patterns will not give us an idea of the possible mutations that the patient presents.

DNA sequencing is critical to identify many human genetic disorders caused by DNA mutations, including cancer. The sequencing has evolved over the years giving rise to a classification in 3 eras. First-generation sequencing that includes Sanger sequencing, which has been the only sequencing method for 30 years. Although it is still used clinically today, large genes are expensive and difficult to deal with complex and multifactorial diseases.

On the other hand, there is the next generation sequencing known as NGS that has many advantages in both speed and cost. Within NGS we find pyrosequencing, a method used in this study that consists of sequencing based on the release of phosphates. This technique has certain advantages

over Sanger: lower cost, greater flexibility and easy automation. Pyrosequencing has high precision, although it does not reach Sanger levels, but without a doubt, its main advantage over previous sequencing is that it is a fast and real-time method. However, its main disadvantage is that sequencing has to be made of short stretches of DNA.

There are other alternative techniques to pyrosequencing that would also be very useful in identifying the mutations analyzed in this study, such as NGS with DNA extension reactions on a chip. Cycle-terminating nucleotides with fluorescent molecules are used in this type of sequencing. The advantage of NGS sequencers (such as Illumina) is the high performance sequencing capacity. There are currently panels prepared for the different mutations that a lung adenocarcinoma can present, in which all the genes included in the molecular guidelines would be analyzed in a single run.

As has been shown in a patient with lung ADC, many things have to be considered. First, the histological pattern is assessed at the time of diagnosis, which gives us an idea of the patient's prognosis. After this, a molecular categorization is carried out according to the guidelines including genes such as EGFR, BRAF and ALK. Including KRAS in molecular categorization will give us more knowledge about tumor behavior, and also the development of the new drug will give an opportunity to the patient.

Considering the frequencies of the mutations and the existence of targeted therapies, 18% may receive a more specific treatment when presenting a mutation in EGFR; 2% will receive directed therapy against ALK and 1.5% will have treatment against BRAF. If we take KRAS into account, and the drug is used in the clinic, 35% of patients will be able to receive it. That is the main reason of why personalized therapy has been one of the most important and impressive developments in cancer treatment.

Specifically, in the last 20 years, a minority of patients with lung cancer have been able to benefit from targeted therapy. Thanks to these new therapies survival has increased. For this reason, studies in basic and translational research that help to understand the molecular biology of cancer and that look for alternative treatments shed a little light on something that seemed unfeasible just a couple of years ago.

6. CONCLUSIONS

KRAS activating mutations are among the most frequent drivers in human cancer. KRAS G12C is the most prevalent mutation of this gene.

Due to the recent development of KRAS inhibitors, it is necessary to genotype KRAS in lung adenocarcinomas using protocols that can distinguish specific alleles since the therapy currently in clinical trials is mutation-specific.

There is no association between histology subtypes of lung adenocarcinoma and mutations in KRAS.

Pyrosequencing is a simple, low-cost and fast genopyting method for this purpose.

REFERENCES

Badve, S., & Kumar, G. L. (2019). *Predictive Biomarkers in Oncology.* Springer.

Bar-Sagi, D., Knelson, E. H., & Sequist, L. V. (2020). A bright future for KRAS inhibitors. *cancer un translation*.

Bos, J. L. (1989). ras Oncogenes in Human Cancer: A Review. *Cancer Research*.

Cage, P. T. (2004). *Pulmonary Pathology.*

Calvayra, O., Pradines, A., Pons, E., Mazières, J., & Guibert, N. (2016). Molecular biomarkers for lund adenocarcinoma. *CrossMark*.

Canon, J., Rex, K., Saiki, A. Y., Mohr, C., Cooke, K., Dahnaeshri Bagal, K. G., . . . Ji-Rong. (2019). The clinical KRAS(G12C) inhibitor AMG 510. *Nature*.

Domagala-Kulawik, J. (2019). New Frontiers for Molecular. *Frontiers in Medicine*.

Drosten, M., Lechuga, C. G., & Barbacid, M. (2014). Ras in epidermal proliferation. *Oncotarget*.

Fletcher, C. D. (2013). *Diagnostic Histopathology of tumor Volume I.* Elsevier.

Garrido, P., Conde, E., & J de Castro, J. G.-R.-A.-R. (2019). Updated guidelines for predictive biomarker testing in advanced non-small-cell lung cancer: a National Consensus of the Spanish Society of Pathology and the Spanish Society of Medical Oncology. *Clinical and Translational Oncology*.

Kessler, D., Gmalch, M., Mantoulidis, A., Martin, L. J., Zoephel, A., & Mayer, M. (2019). Drugging an undruggable pocket on KRAS. *PNAS*.

Kumar, V., Abbas, A. K., & Aster, J. C. (2012). *Human Pathology*. Elsevier.

Pecorino, L. (2012). *Molecular Biology*. Oxford.

Qiagen. (2015). *therascreen® KRAS Pyro® Kit*.

Qiagen. (2020, Enero 20). Retrieved from https://www.qiagen.com/es/products/discovery-and-translational-research/pyrosequencing/instruments/pyromark-q24/?clear=true#orderinginformation

Weinberg, R. A. (2014). *The biology of Cancer*. Carland Science.